GEOPHYSICAL RESEARCH LETTERS, VOL. ???, XXXX, DOI:10.1029/,

Fast Thermospheric Wind Jet At The Earth's Dip Equator

Huixin Liu

Earth and Planetary Science Division, Hokkaido University, Japan

Shigeto Watanabe

Earth and Planetary Science Division, Hokkaido University, Japan

Tsutomu Kondo

Earth and Planetary Science Division, Hokkaido University, Japan

H. Liu, and S. Watanabe, and Tsutomu Kondo, Earth and Planetary Science Division, Hokkaido University, Sapporo 060-0810, Japan (huixin@ep.sci.hokudai.ac.jp)

The thermospheric zonal wind forms a fast wind jet at the Earth's dip equator instead of the geographic equator. This remarkable feature is revealed in two sets of independent observations made two decades apart. One is from the CHAMP satellite during the year of 2002 and the other is from the DE-2 satellite during Aug. 1981 – Feb. 1983. Both observations show that this wind jet is eastward at night with speed reaching 150 ms^{-1}, and westward around noon with speed over 75 ms^{-1}. These fast wind jets are observed during local times of fully developed equatorial ionization anomaly (EIA). On the other hand, a channel of slow wind is found on the dip equator during the period of 05–08 MLT, which corresponds to local times before the EIA develops. These features strongly suggest the ion drag being the principle cause for shifting the wind jet from the geographic equator to the dip equator.

1. Introduction

The Earth's thermosphere covers the region from about 80 km to 500 km altitude depending on latitude and local time. Its thermal dynamics are mainly controlled by the solar EUV/UV heating at low to middle latitudes. From this point of view, the thermosphere forms a high density bulge at the subsolar point and a density hole at the midnight. This distribution builds up pressure gradient directing from noon to midnight, which drives thermospheric winds. The gross structures of the neutral density and wind are described well by empirical models like MSIS and HWM, with a density maximum at the subsolar point and the strongest wind at the geographic equator for equinoxes or seasonally averaged case [*Picone et al.*, 2002; *Hedin et al.*, 1996]. However, satellite observations have revealed significant deviations from these gross features. In particular, the equatorial ionization anomaly (EIA) [*Namba and Maeda*, 1939; *Appleton*, 1946] has been demonstrated to strongly modify the classical picture of the thermosphere. For instance, the neutral density has been found to form a minimum at the dip equator flanked by two maxima on both sides [*Hedin and Mayr*, 1973; *Liu et al.*, 2005, 2007], resembling the latitudinal structure of EIA.

The zonal wind has been reported by *Raghavarao et al.* [1991] and *Coley et al.* [1994] to blow strongest at the Earth's dip equator instead of the geographic equator. Both studies used the DE-2 measurements during 1981-1983. Due to the lack of neutral wind observations at upper thermospheric altitudes ($\sim$ 400 km), this important feature has not been corroborated by independent measurements thereafter. Recently, the CHAMP satellite has been providing in situ high-resolution thermospheric wind observations in the cross-track direction with a global coverage [*Liu et al.*, 2006; *Lühr et al.*, 2007; *Förster et al.*, 2008]. A comparison between the

CHAMP-derived zonal wind and that predicted by the HWM model in equatorial regions has revealed satisfactory agreement in most local times [*Liu et al.*, 2006]. Since the HWM model prediction at the altitude of CHAMP is mainly based on DE-2 measurements, the comparison was in fact a comparison between the CHAMP and DE-2 measurements. In this paper, we investigate the latitudinal structure of zonal winds at low and middle latitudes. By comparing the CHAMP and DE-2 measurements, we aim to examine the global feature of wind jet with independent observations.

2. Data

Two sets of independent thermospheric zonal wind measurements are utilized in this study. One is the 10-s averaged data from the CHAMP satellite and the other is the 16-s averaged data from the DE-2 satellite. CHAMP is in a near-circular orbit with an inclination of $87.3°$. The average altitude in the year of 2002 is about 410 km. Its orbital plane precesses through all local times every 3 months. It effectively probes the in-situ wind with an accuracy of ~ 20 ms^{-1}. The inclination of DE-2 satellite is $90°$ and has its perigee at around 300 km. The accuracy of the wind measurements from DE-2 is $\sim 10 - 20$ ms^{-1}. It samples through all local times every 6 months. Readers are referred to *Liu et al.* [2006] and *Spencer et al.* [1981] for details concerning the derivation procedure and related errors about these data.

The chosen data periods are Jan. 2002-Dec. 2002 and Aug. 1981–Feb. 1983 for CHAMP and DE-2, respectively. The year of 2002 is chosen for CHAMP, since the average solar radio flux value (F10.7=179) is comparable to that for DE-2 (F10.7=166). Data during very active periods (Kp≥ 5) are excluded in the following analysis.

3. Results

The seasonally averaged zonal wind distribution in the frame of geographic latitude vs. geographic longitude is presented in Figure 1 for the period of 18–24 MLT. The upper panel is for CHAMP and the lower one for DE-2. The solid line depicts the dip equator. We see that the zonal wind blows eastward at low to middle latitudes as observed by both satellites. The wind velocity peaks in the equatorial region and decreases towards higher latitudes. An interesting feature stands out prominently. That is, a banded structure forms along the solid line. In this band, the maximum wind velocity is found at the Earth's dip equator, instead of the geographic equator. The wind speed amounts to nearly $150\,\mathrm{ms}^{-1}$, twice as that near $\pm 25°$ magnetic latitude. Both the CHAMP and DE-2 observations reveal nearly identical latitudinal pattern.

Figure 1

We now examine the wind pattern from an alternative persective. Figure 2 illustrates the zonal wind distribution in the frame of magnetic dip latitude vs. magnetic local time in quasi-dipole coordinates. Although some differences exist in the mean values of the wind and also in the local times of westward-to-eastward wind reversal and the second maximum (which will be addressed later), both CHAMP and DE-2 observations reveal fairly similar wind patterns. The wind at equatorial latitudes blows eastward during night and westward before afternoon (14 MLT for CHAMP and 16 MLT for DE-2). Towards higher latitude, the morning wind reversal from eastward to westward occurs progressively at earlier local times. For instance, the reversal is at $\sim$02 MLT near $\pm 30°$ latitude in comparison to 05–06 MLT at the dip equator. This leads to a pronounced triangle shape in the 2-D distribution of the wind shown in Figure 2. On the nightside, the latitudinal variation of the wind exhibits a maximum at the dip equator (better seen in the black curves in the right panels of Figure 2). This fast wind jet continues throughout

Figure 2

the time of eastward wind. During 05–08 MLT, both observations show a minimum westward flow at the dip equator sandwiched by faster westward flow at middle latitudes (see pink curves in Figure 2). After 09 MLT, however, the strongest westward flow is again found at the dip equator (blue curves in Figure 2). In summary, the wind forms a fast eastward jet at the dip equator during 18–05 MLT, and a fast westward jet after 09 MLT. During 05–08 MLT, the dip equator becomes a channel of slow wind. There is good agreement on these trends revealed by CHAMP and DE-2 observations.

4. Discussion

The above analysis of the latitudinal structure of the thermospheric zonal wind has revealed a fast wind jet at the Earth's dip equator in both the CHAMP and DE-2 observations (see Figure 1). It is remarkable to see how similar this structure is in two independent datasets obtained two decades apart with totally different instruments. The CHAMP probes the in-situ neutral wind with a tri-axis accelerometer, while the DE-2 measured the wind with a wind and temperature spectrometer. The principles of these instruments are completely different as described in *Liu et al.* [2006] and *Spencer et al.* [1981]. Furthermore, the neutral wind varies significantly with location, season, solar and geomagnetic conditions [*Liu et al.*, 2004, 2006]. Given these intrinsic variability and the totally different observing techniques, the consistency between latitudinal structures revealed in the two datasets is striking. The CHAMP observations corroborate the DE-2 measurements, and strongly confirm the existence of the fast wind jet and and its stable location at the dip equator.

This wind jet along the Earth's dip equator instead of the geographic equator demonstrates strong magnetic control of the thermospheric dynamic. In the upper atmosphere at low latitudes, the atmospheric pressure gradient is the primary driver of the neutral wind, with the ion drag being an important impeding force. It regulates the neutral wind considerably [*Rishbeth*, 1972]. With the development of the EIA structure in the equatorial ionosphere after ~ 09 MLT, the plasma density forms a trough at the dip equator [*Balan and Bailey*, 1995]. This consequently leads to lower ion drag, which facilitates faster wind to flow at the dip equator. During the period of 05–08 MLT, however, the EIA structure disappears and a peak of the plasma density forms at the dip equator instead of a trough [*Lin et al.*, 2007]. This causes the ion drag to peak at the dip equator as well, hence to slow down the zonal wind considerably. As a result, the dip equator becomes a channel of slow flow instead of fast flow. The local time variation of the wind jet examined in section 3 shows this is exactly the case. Fast wind jet is found at the dip equator during 18–05 MLT and after 09 MLT, while slow wind presents during 05–08 MLT. These observations strongly suggest the ion drag being the principle cause for shifting the fast wind jet from the geographic equator to the dip equator.

Besides the similar latitudinal structure revealed by CHAMP and DE-2, we note that an apparent difference is seen in the occurring time of westward-to-eastward wind reversal and the second wind maximum after midnight. The reversal is around 13–14 MLT for CHAMP, while around 16–17 MLT for DE-2. The second wind maximum is around 01 MLT for CHAMP, while near 03 MLT for DE-2 (see Figure 2). Along with differences in the mean values of the wind speed, they likely arise from several sources as previously pointed out in [*Liu et al.*, 2006]. First, seasonal average. Due to the slow precessing rate of DE-2's orbital plane, the DE-2 dataset suffers strongly from the locking between local time and season. The midnight/noon sectors were predominantly sampled around equinoxes, while the dawn/dusk sectors around solstices. Since

CHAMP transverses all local times every 3 months, each local time is equally sampled in four seasons in one year. Second, altitude average. The altitude of DE-2 measurements ranges from 200–700 km, while CHAMP measurements are collected within a much smaller altitude range between 400–430 km. Third, some discrepancies arising from different instruments used by DE-2 and CHAMP cannot be ruled out. These differences between the two sets of measurements may have contributed to the above-mentioned discrepancies.

Finally, it is worth pointing out that except for at $\sim$20 MLT, no bands of slow wind near $\pm 25°$ latitude is discernible (see e.g., Figure 1). This is different from that reported in *Raghavarao et al.* [1991]. In their study, *Raghavarao et al.* examined the latitudinal variation of the wind orbit by orbit instead of in a statistical manner as we do here. As shown in Figure 1 of *Raghavarao et al.* [1991], for instance, the wind peak at the dip equator is very prominent and broad, with a width about $20°$ in latitude. But the wind trough near $\pm 25°$ latitude is much narrower ($\sim 7°$). Furthermore, the location of the wind trough is expected to be highly variable with season, following that of the EIA crests. Therefore, it is quite likely that this narrow trough structure with shallow magnitude has been smeared out in statistical analysis, as a consequence of combing measurements in different season, longitudes and local times. The statistical analysis of the DE-2 wind in *Coley et al.* [1994] has revealed no band of slow wind either, consistent with our results. The exception around 20 MLT (see right panels of Figure 2), with a subtle signature of slow winds near $\pm 20°$ magnetic latitude, is likely due to the post-sunset enhancement of the EIA [*Balan and Bailey*, 1995]. This enhanced EIA leads to a much more significant depression of the zonal wind in crest regions than at other local times, which could have survived the statistical averages.

In summary, both the CHAMP and DE-2 observations reveal a fast wind jet at the Earth's dip equator instead of the geographic equator, demonstrating the strong magnetic control of the neutral dynamics via ion drag.

Acknowledgments. We thank W. Köhler for processing the CHAMPdata. The work of HL is supported by the JSPS foundation. The CHAMP mission is supported by the German Aerospace Center (DRL) in operation and by the Federal Ministry of Education and Research (BMBF) in data processing.

References

Appleton, E. V. (1946), Two anomalies in the ionosphere, *Nature*, *157*, 691.

Balan, N., and G. J. Bailey (1995), Equatorial plasma fountain and its effects: Possibility of an additional layer, *J. Geophys. Res.*, , *100*, 21,421–21,432, doi:10.1029/95JA01555.

Coley, W. R., R. A. Heelis, and N. W. Spencer (1994), Comparison of low-latitude ion and neutral zonal drift using DE2 data, *J. Geophys. Res.*, *99*, 341–348.

Förster, C., S. Rentz, W. Köhler, H. Liu, and S. E. Haaland (2008), IMF dependence of high-latitude thermospheric wind pattern derived from CHAMP cross-track measurements, *Ann. Geophys.*, *26*, 1581–1595.

Hedin, A. E., and H. G. Mayr (1973), Magnetic control of the near equatorial neutral thermosphere, *J. Geophys. Res.*, *78*, 1688–1691.

Hedin, A. E., et al. (1996), Empirical wind model for the upper, middle and lower atmosphere, *J. Atmos. Solar-Terr. Phys.*, *58*, 1421–1447.

Lin, C. H., J. Y. Liu, T. W. Fang, P. Y. Chang, H. F. Tsai, C. H. Chen, and C. C. Hsiao (2007), Motions of the equatorial ionization anomaly crests imaged by FORMOSAT-3/COSMIC, *Geophys. Res. Lett.*, *34*, L19101, doi:10.1029/2007GL030741.

Liu, H., H. Lühr, V. Henize, and W. Köhler (2005), Global distribution of the thermospheric total mass density derived from CHAMP, *J. Geophys. Res.*, *110*, A04301, doi: 10.1029/2004JA010741.

Liu, H., H. Lühr, S. Watanabe, W. Köhler, V. Henize, and P. Visser (2006), Zonal winds in the equatorial upper thermosphere: decomposing the solar flux, geomagnetic activity, and seasonal dependencies, *J. Geophys. Res.*, *111*, A09S29, doi:10.1029/2005JA011415.

Liu, H., H. Lühr, and S. Watanabe (2007), Climatology of the Equatorial Mass Density Anomaly, *J. Geophys. Res.*, *112*, A05305, doi:10.1029/2006JA012199.

Liu, L., X. Luan, W. Wan, J. Lei, and B. Ning (2004), Solar activity variations of equivalent winds derived from global ionosonde data, *J. Geophys. Res.*, A12305, doi: 10.1029/2004JA010574.

Lühr, H., S. Rentz, P. Ritter, H. Liu, and K. Häusler (2007), Average thermospheric wind patterns over the polar regions, as observed by CHAMP, *Ann. Geophys.*, *25*, 1093–1101.

Namba, S., and K.-I. Maeda (1939), *Radio wave propagation*, 86 pp., Corona Publishing, Tokyo.

Picone, J. M., A. E. Hedin, D. P. Drob, and A. C. Aikin (2002), NRLMSISE-00 empirical model of the atmosphere: Statistical comparisons and scientific issues, *J. Geophys. Res.*, *107*, 1468, doi:10.1029/2002JA009430.

Raghavarao, R., L. E. Wharton, N. W. Spencer, H. G. Mayr, and L. H. Brace (1991), An equatorial temperature and wind anomaly (ETWA), *Geophys. Res. Lett.*, *18*(7), 1193–1196.

Rishbeth, H. (1972), Thermospheric winds and the F-region: A review, *J. Atmos. Terr. Phys.*, *34*, 1–47.

Spencer, N. W., L. E. Wharton, H. B. Niemann, A. E. Hedin, G. R. Carignan, and J. C. Maurer (1981), The Dynamics Explorer wind and temperature spectrometer, *Space Sci. Instrum.*, *5*, 417–428.

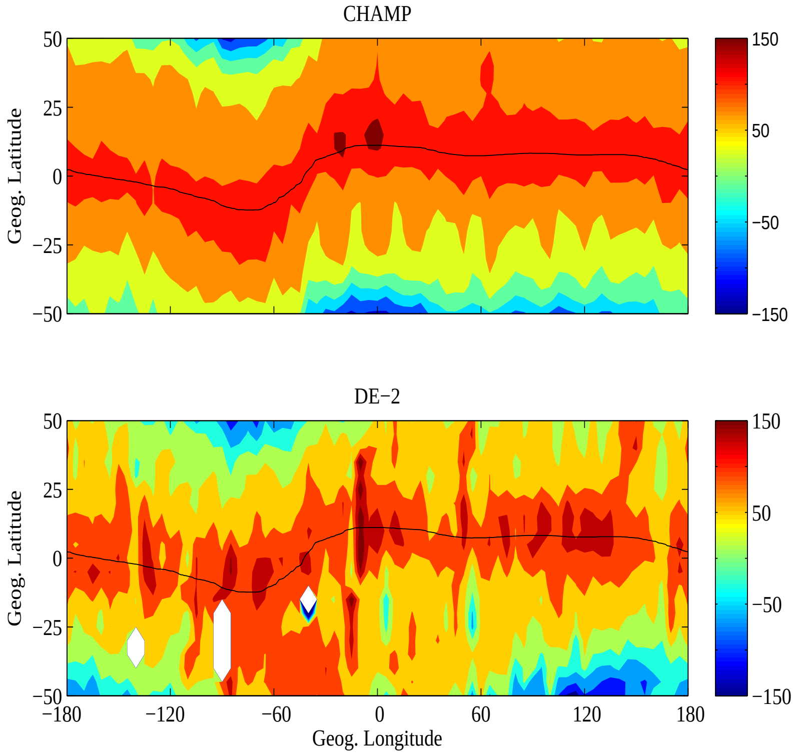

Figure 1. Distribution of the seasonally averaged zonal wind velocity (in unit of ms^{-1}) in the frame of geographic longitude vs. geographic latitude during periods of 18–24 MLT. Positive means eastward. The upper panel is for CHAMP and the lower panel for DE-2. The solid line indicates the dip equator. Note the banded structure along the dip equator, where the fastest wind flows.

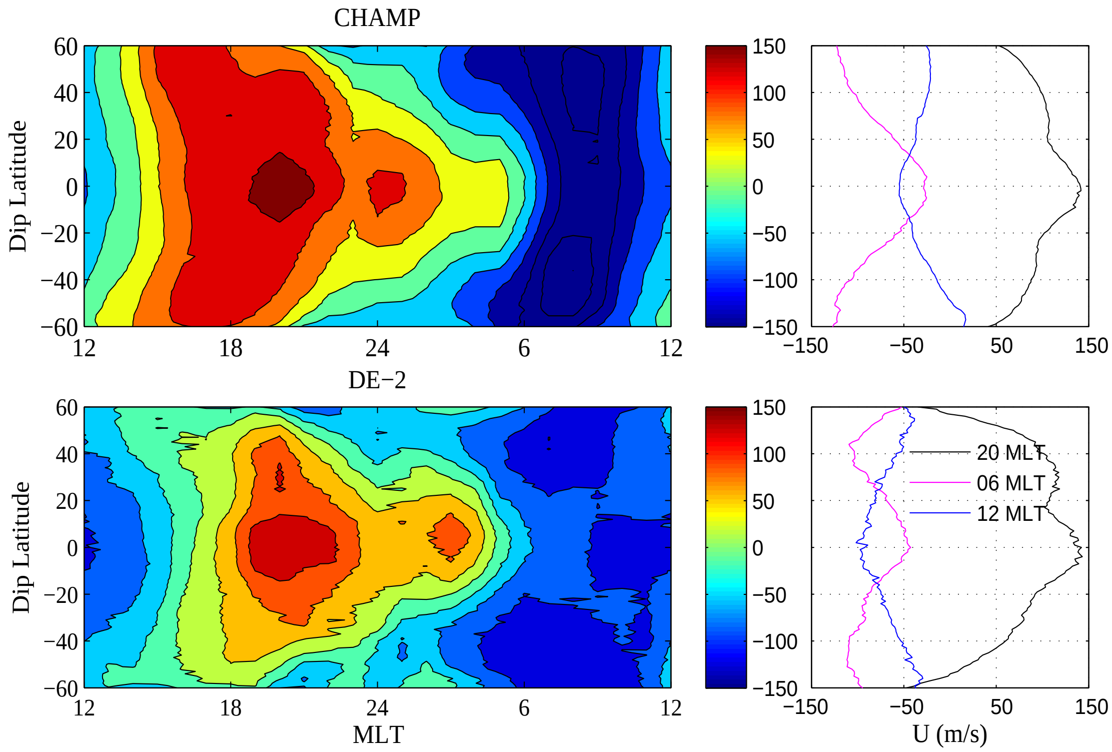

Figure 2. Distribution of the seasonally averaged zonal wind velocity (in unit of m s^{-1}) in the frame of magnetic dip latitude vs. magnetic local time in quasi-dipole coordinates. Positive means eastward. The upper row is for CHAMP and the lower row for DE-2. Corresponding latitudinal profiles at 06 MLT, 12 MLT, and 20 MLT are shown in the right panels.